Beyond the Crack Size Criterion: The Effect of a Fracture on Calcium Depletion of Cementitious Materials

F.H.Heukamp, M.Mainguy & F.-J. Ulm
Massachusetts Institute of Technology, Cambridge, Massachusetts

The importance of cracks on the depletion of cementitious materials is usually assumed to be high. In this paper, similarity properties of diffusion dominated mass transport coupled with Calcium dissolution in cracked cementitious materials are presented. Together with model-based simulations that confirm the self-similar properties of diffusion dominated mass transport in the fracture, it is shown that diffusion dominated transport does not significantly accelerate the Calcium leaching of the bulk material. In turn, a first estimate of the effect of Calcium leaching on the brittleness of the material predicts an increase in ductility.

1 INTRODUCTION

Cracks and fractures in low permeable porous materials have long been suggested to affect the overall mass transport and related chemo-physical phenomena, such as phase-change, dissolution and sorption processes. And in some industrial concrete applications, cracks are considered critical to the long-term dimensional stability of structures. This is the case in e.g. nuclear waste disposal structures, subjected to the critical design scenario of calcium leaching by permanently renewed water (Adenot et al. 1999). For containment structures, critical crack size criteria are often suggested as a quality control to ensure the durability performance of concrete containers, barriers and encasement. This paper, however, argues that the crack opening is not the most critical parameter affecting the overall degradation kinetics of the material, if the mass transport through the fracture is diffusion driven. Our argument is a dimensional one.

2 REFERENCE PROBLEM OF CALCIUM LEACHING IN CRACKED POROUS MATERIALS

2.1 Idealized Geometry and Problem

We consider a semi-infinite domain $y > 0$, divided by a semi-infinite fracture channel of constant width $2b$ (see Fig.1), which is much smaller than the fracture length.

The cementitious material is assumed a two-phase porous material, consisting of a solid skeleton and an interstitial pore solution. Calcium (Ca), the modeled mineral, is present in both phases. The Calcium leaching process is initiated as the Ca-concentration
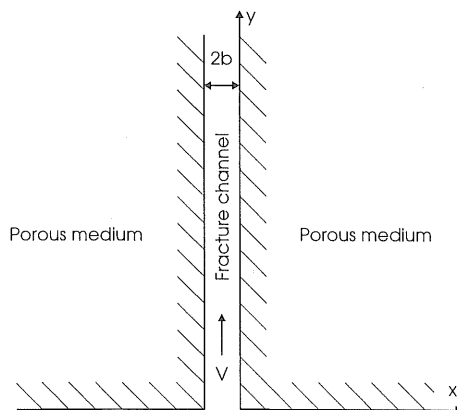

Figure 1: Fracture-Porous medium system. A diffusion process occurs in the fracture coupled with diffusion and dissolution in the porous medium

in the interstitial solution is lower than the equilibrium concentration between pore solution and solid. We assume that the transport process in both phases is purely diffusive. The diffusion process in the matrix is assumed to occur only in the x−direction, and is driven by a zero solute concentration boundary condition prescribed at the inlet of the channel at $y = 0$ over the fracture width. The effect of advective transport, which can play a significant role in low permeable materials (Walton and Seitz 1992), will be addressed at the end of the paper.

2.2 Dimensional Analysis

The simplified reference problem is the one of two orthogonal one-dimensional diffusion problems cou-

pled through the continuity of the Calcium concentration at the interface $x = 0$, and the influx of solute from the matrix into the fracture channel. The governing equations of the problem are (Mainguy and Ulm 2001):

1. The mass conservation in the porous material i.e. for $x, y, t > 0$:

$$\frac{\partial(\phi\rho_m)}{\partial t} + \frac{\partial m_m}{\partial t} - \frac{\partial}{\partial x}\left(\phi D_m \frac{\partial \rho_m}{\partial x}\right) = 0; \quad (1)$$

and in the fracture of constant fracture width $2b$, i.e. for $y, t > 0$:

$$\frac{\partial \rho_f}{\partial t} + \frac{\partial}{\partial y}\left(-D_f \frac{\partial \rho_f}{\partial y}\right) + \frac{q_x}{2b} = 0; \quad (2)$$

where $\rho_m = \mathcal{M}c$ and $\rho_f = \mathcal{M}c$ denote the concentration of the Calcium ions, with $\mathcal{M}$ the molar mass of Calcium, and c the molar concentration; m_m stands for the apparent volume mass of the same mineral bound in the skeleton, and $\partial m_m / \partial t$ is the skeleton mass variation due to the leaching process. The solvent in the porous continuum is assumed at rest, so that the solute mass transport occurs through molecular diffusion, described by Fick's first law (term of the form $-\phi D_m \partial \rho_m / \partial x$). The flux $-D_f \partial \rho_f / \partial y$ accounts for the diffusive mass transport in the fracture. Finally, if we assume that the fracture width $2b$ and the porosity ϕ of the solid matrix are not changed due to the dissolution process, the diffusion coefficient in the solid matrix D_m and the hydrodynamic coefficient in the fracture D_f can be considered as constant.

2. The jump $[q_x]$ in solute flux over the fracture of opening $2b$, which results from the flux of matter from the porous material in the the fracture channel. Taken the symmetry of the problem with regard to the fracture channel, the flux jump reads:

$$[q_x] = -2\phi D_m \frac{\partial \rho_m}{\partial x}|_{x=0} \quad (3)$$

3. The chemical dissolution law: At chemical equilibrium, the molar concentration c of the Calcium in the interstitial pore solution is equal to the chemical equilibrium concentration c_{eq}. If we note $\rho_{eq} = \mathcal{M}c_{eq}$ the corresponding volume mass density at chemical equilibrium, and m_m the apparent volume mass of the same mineral bound in the skeleton, the instantaneous dissolution of the mineral bound in the skeleton is described by (Mainguy and Coussy 2000):

$$m_m \geq 0 ; \quad \rho_m - \rho_{eq} \leq 0 ; \quad m_m(\rho_m - \rho_{eq}) = 0 \quad (4)$$

4. The initial conditions, at time $t = 0$, in the matrix for $x, y > 0$:

$$\rho_m(x, y, t = 0) = \rho_{eq}, \ m_m(x, y, t = 0) = m_0 \quad (5)$$

, and in the fracture for $y \geq 0$:

$$\rho_f(y, t = 0) = \rho_m(x = 0, y, t = 0) = \rho_{eq} \quad (6)$$

where m_0 is the initial apparent volume mass density of the mineral bound in the skeleton.

5. The boundary condition at the fracture inlet:

$$\rho_f(y = 0, t) = 0, \quad t > 0 \quad (7)$$

6. The continuity of the solute concentration between the fracture and the matrix:

$$\rho_f(y, t) = \rho_m(x = 0, y, t), \quad y, t > 0. \quad (8)$$

A dimensional analysis shows that the three dimensionless unknown of the problem, $\bar{\rho}_f, \bar{\rho}_m$ and $\bar{m}_m$ depend on four invariants (Mainguy and Ulm 2001):

$$\bar{\rho}_f = \frac{\rho_f}{\rho_{eq}} = \mathcal{F}(\bar{y}, \bar{t}, \varepsilon); \ \bar{\rho}_m = \frac{\rho_m}{\rho_{eq}} = \mathcal{G}(\bar{x}, \bar{y}, \bar{t}, \varepsilon) \quad (9)$$

$$\bar{m}_m = \frac{m_m}{m_0} = \mathcal{H}(\bar{x}, \bar{y}, \bar{t}, \varepsilon) \quad (10)$$

with:

$$\bar{y} = y\sqrt{\frac{1}{D_f(2b/\phi)}}\left(\frac{D_m}{t}\right)^{1/4} \quad (11)$$

$$\bar{x} = \frac{x}{2\sqrt{D_m t}}; \ \bar{t} = \frac{\sqrt{D_m t}}{b/\phi}; \ \varepsilon = \frac{\phi \rho_{eq}}{m_0} \quad (12)$$

The dimensionless coordinate $\bar{y}$ characterizing the diffusion process in the fracture indicates a self-similar time-space relation proportional to the quadratic root of time in a diffusion controlled mass transport in the fracture (i.e., $y(t) \propto t^{1/4}$). The $t^{1/4}$−dependency of the diffusion controlled mass transport translates the fact that the mass transport is governed by two coupled 1D-diffusion process, one in the y−direction through the fracture, the other in the x−direction through the bulk material.

The remaining invariants $\bar{x}$, $\bar{t}$ and ε, defined by (12), have the following physical significance: The Boltzmann variable $\bar{x}$ characterizes the diffusion process in the porous material. The normalized time $\bar{t}$ relates the solute diffusion length $2\sqrt{D_m t}$ in the porous material to the fracture width, or more precisely to an effective fracture width, magnified by the inverse of the bulk porosity, $2b/\phi$. This invariant introduces a gauge time τ_b:

$$\bar{t} = \left(\frac{t}{\tau_b}\right)^{1/2}; \quad \tau_b = \frac{(b/\phi)^2}{D_m} \qquad (13)$$

Finally, invariant ε can be interpreted as a macroscopic solubility constant of the dissolution process, which relates at equilibrium the apparent chemical equilibrium mineral mass density in solution, $\phi\rho_{eq}$, to the initial mineral mass density, m_0, in the solid phase. These invariants provide a means to study the asymptotic behavior of diffusion dominated mass transport in the fracture.

2.3 Large Time Asymptotic Behavior

The one-dimensional problem of diffusion and dissolution in the porous medium with a zero boundary condition prescribed at $x = 0$, which is similar to a Stephan problem is characterized by the presence of a sharp dissolution front or wave propagating at finite velocity through the bulk material. The position x_d of the dissolution front depends on the square root of time, and is given by (Mainguy and Coussy 2000):

$$x_d(t) = 2\bar{x}_d(\varepsilon)\sqrt{D_m t} \qquad (14)$$

where $\bar{x}_d = \bar{x}_d(\varepsilon)$ is the solution of the following equation:

$$\varepsilon \exp(-\bar{x}_d^2) - \sqrt{\pi}\bar{x}_d \mathrm{erf}(\bar{x}_d) = 0 \qquad (15)$$

The dissolution front located by x_d (see figure 2) separates a completely degraded zone where the solid mineral is entirely dissolved ($m_m = 0$ for $x < x_d$), from an undegraded zone where the solid mineral is at the initial value ($m_m = m_0$ for $x > x_d$).
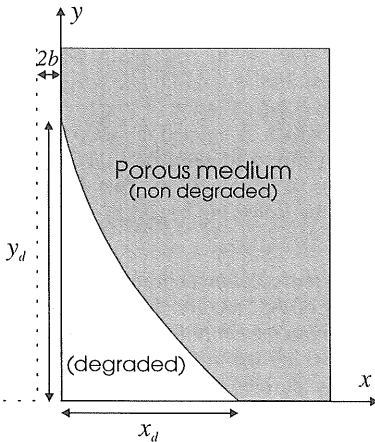

Figure 2: Definition of the degradation profile with x_d and y_d the degradation lengths in the x-direction and along the fracture channel.

The instantaneous dissolution process implies also the existence of a finite degraded depth along y at the fracture-solid matrix interface ($x = 0$). This degraded depth, to which we will refer as fracture degradation length, is noted y_d and is shown in figure 2. For large times $\bar{t} \gg 1 \leftrightarrow t \gg \tau_b$, for which the mass transport in the fracture is in a quasi-steady state condition with the solute influx from the surrounding porous medium, the solution of the problem becomes independent of the normalized time $\bar{t}$, and (9) and (10) reduces to:

$$\bar{\rho}_f = \mathcal{F}(\bar{y}, \varepsilon); \quad \bar{\rho}_m = \mathcal{G}(\bar{x}, \bar{y}, \varepsilon); \quad \bar{m}_m = \mathcal{H}(\bar{x}, \bar{y}, \varepsilon) \qquad (16)$$

This implies the following form of y_d for the limit case at large times:

$$t \gg \tau_b: \quad y_d^{dif}(t) = \bar{y}_d^{dif}(\varepsilon)\sqrt{D_f \frac{2b}{\phi}}\left(\frac{t}{D_m}\right)^{1/4} \qquad (17)$$

where $\bar{y}_d^{dif}(\varepsilon)$ is the dimensionless front position function, which —similarly to $\bar{x}_d(\varepsilon)$ in (14)— links the fracture degradation length to the macroscopic solubility ε. Eq. (17) indicates that the fracture degradation length develops as a linear function of the quadratic root of time ($y_d^{dif} \propto t^{1/4}$), and is scaled by the square root of the crack opening ($y_d^{dif} \propto \sqrt{2b/\phi}$). For large times $t \gg \tau_b$, due to the $t^{1/4}-$ dependency, the diffusion through the fracture slows down in time, in comparison with the one dimensional degradation process, which penetrates with the square root of time into the uncracked bulk material. The solute diffusion through the fracture, therefore, is not expected to significantly increase the chemical degradation of the material.

Finally, the relevance of the asymptotic solutions (17) and (22) of the studied reference problem is defined by the gauge time τ_b, which increases with $(b/\phi)^2/D_m$. For concrete applications in nuclear waste containment, maximum crack openings due to shrinkage are on the order of $2b \leq 1$ mm, the porosity is on the order of $\phi = 0.1 - 0.5$, and the calcium diffusivity is $\phi D_m \approx 10^{-12} - 10^{-11}$ m^2/s (Tognazzi 1998). This gives a rough estimate of $\tau_b \leq 30$ days, which implies that the asymptotic expression (17) is relevant for assessing the effect of cracks on the chemical degradation process of concrete at the time-scale of nuclear waste disposal of $300 - 1000$ years.

3 SIMILARITY PROPERTIES OF 'REAL' CALCIUM LEACHING IN CRACKED CEMENT-BASED MATERIALS

'Real' calcium leaching in cement-based materials

is a multi-stage process, which involves the successive demineralization of different constituents of the mineral matrix at specific calcium ion concentrations in the interstitial pore solution (see *e.g.* (Berner 1988); (Adenot and Buil 1992); (Reardon 1992)). This leads to multiple dissolution fronts and an increase in porosity ϕ, which were not considered in the 1D single phase demineralization process analyzed before. The non-linearity of the process requires numerical simulations.

3.1 Model, Model Parameters and Finite Element Implementation of Calcium Leaching in Cracked Cement-based Materials

The model we consider is a two-dimensional extension of the 1D diffusion-dissolution problem , given by (1) to (4). The coupled diffusion-dissolution process in the uncracked cement-based material is described by the molar mass balance equation:

$$\frac{\partial}{\partial t}(\phi c) + \frac{\partial s}{\partial t} - \nabla \cdot (\mathbf{D}_{eff} \cdot \nabla c) = 0 \qquad (18)$$

and a chemical equilibrium condition of the multi-stage dissolution process:

$$s - g(c) = 0 \qquad (19)$$

In (18), $c = \rho_m/\mathcal{M}$ is the molar concentration of the calcium in the interstitial pore solution. It is related through the chemical equilibrium condition (19), which replaces (4), to the molar concentration of calcium, $s = m_m/\mathcal{M}$, bound in the different minerals of the solid matrix. $\mathbf{D}_{eff}$ is the tensor of effective ion diffusivities of calcium in the porous material, and depends on the porosity ϕ, which in turn depends on the solid concentration, and thus on the solid molar concentration s. Functions $\mathbf{D}_{eff} = D_{eff}(\phi)\mathbf{1}$ ($\mathbf{1}$ = second order unit tensor), $\phi = \phi(s)$ and the chemical equilibrium condition (19) are fully described in (Mainguy and Coussy 2000) for a cement paste of water:cement ratio equal to $w/c = 0.4$.

Analogously, the mass balance in the fracture is written in molar form:

$$\frac{\partial c}{\partial t} - \nabla \cdot (\mathbf{D}_f \cdot \nabla c) = 0 \qquad (20)$$

In contrast to the simplified 1D-model (i.e., Eq. (2)), the calcium influx (3) from the surrounding porous material need not to be considered explicitly, but is handled in the 2D-model through the continuity condition at the fracture-matrix interface. The tensor of hydrodynamic dispersion coefficients in the fracture $\mathbf{D}_f$ accounts for the molecular diffusion in the

fracture, but also for the fluid mechanical dispersion due to the transversal variations of the fluid velocity across the fracture ('Taylor' dispersion), even though molecular diffusion in concrete applications dominates over fluid dispersion. Here, $\mathbf{D}_f = D^*\mathbf{1}$, with D^* the isotropic calcium diffusion coefficient in free water. In the numerical investigation, the calcium diffusion coefficient is fixed at an upper bound value of $D^* = 2 \times 10^{-9}$ m^2 s^{-1}.

Equations (18)–(20) are solved using the Finite Element Method based on a variational formulation of the problem with s and c as principal unknowns, linked by the chemical equilibrium condition (19) at the fracture-matrix interface. In the uncracked matrix, the use of $s = s(\mathbf{x},t)$ as principal unknown within low order finite elements (linear basis functions), together with an implicit time integration scheme and mass lumping (see, *e.g.* (Hughes 1987)), ensures an accurate oscillation-free determination of the position of the dissolution fronts in time and space. In the fracture, where the bound calcium concentration has no significance, the calcium concentration $c = c(\mathbf{x},t)$ is employed as principal unknown. Finally, the continuity of both the calcium concentration and the normal calcium flux in the two-field discretization (s in the matrix, c in the fracture) is realized through the implementation of the chemical equilibrium condition (19) into two-node penalty elements with c_i as degree of freedom in the fracture, and s_i as degree of freedom on the matrix side. Space and time step increments are selected such to avoid the effects of numerical dispersion and overshoot, which may result from high fluid flow velocity in the fracture (see, for instance, (Sun 1996)).

Given the symmetry of the fracture channel and surrounding matrix, the finite element simulations are realized on half of the geometry displayed on figure 1, with a zero flux boundary condition applied along the fracture center line (symmetry), and on the top and right sides of the rectangular geometry (far field conditions). Initial conditions correspond to a calcium molar solid concentration of $s(\mathbf{x},t=0) = 14.7 \times 10^3$ mol/m^3, which is related by chemical equilibrium (*i.e.*, Eq. (19)) to an interstitial calcium concentration of $c(\mathbf{x},t=0) = 21$ mol/m^3. Two degradation scenarios with the following boundary conditions are studied:

– $\mathcal{B}1$: A zero calcium concentration prescribed at the inlet of the fracture. This case corresponds precisely to the simplified 1D-degradation scenario, for which the similarity properties were previously derived. In this case, the solid material diffusivity in the y-direction is set to zero (*i.e.*, $D_{eff}^{yy} = \mathbf{e}_y \cdot \mathbf{D}_{eff} \cdot \mathbf{e}_y = 0$), which implies a zero flux boundary condition along $y = 0$ and $x > b$.

– $\mathcal{B}2$: A zero calcium concentration prescribed along $y = 0$ on both solid material and fracture inlet.

This case corresponds to the realistic degradation process of cracked porous media, and will allow us to analyze the validity of asymptotic behaviors previously identified for the idealized degradation process. In this case, the solid material diffusivity is assumed isotropic, $\mathbf{D}_{eff} = D_{eff}\mathbf{1}$.

3.2 Discussion of Results of Model-Based Simulation

An application of the model gives the following results: For boundary conditions $\mathcal{B}1$, figure 3 displays the evolution of the fracture degradation length y_d^{dif} versus the quadratic square root of time $t^{1/4}$ for different fracture openings, ranging from $2b = 0.1$ mm to $2b = 1$ mm. Figure 4 shows the same results, but in
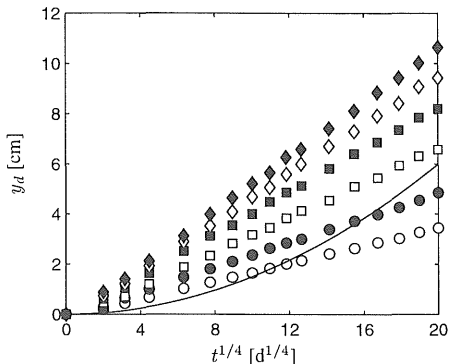
Figure 3: Fracture degradation length y_d versus $t^{1/4}$ for a pure diffusive mass transport in the fracture, a zero solid matrix diffusivity in the y-direction and different crack openings $2b$: $\bigcirc$ = 0.1 mm; $\bullet$ = 0.2 mm; $\square$ = 0.4 mm; $\blacksquare$ = 0.6 mm; $\Diamond$ = 0.8mm; $\blacklozenge$ = 1 mm. The solid line corresponds to the one dimensional degradation of the solid matrix ($x_d = 1.5 \times 10^{-2}\sqrt{t}$ with t in days and x_d in cm) [Boundary Condition $\mathcal{B}1$]

a plot of $y_d^{dif}/\sqrt{2b}$ versus $t^{1/4}$ for the maximum and minimum crack opening. Noting that y_d^{dif} characterizes the position of the Portlandite dissolution front, which is the first mineral dissolved in cause of 'real' calcium depletion, the numerical results confirm the similarity properties of the asymptotic solution (17), i.e.:

- The asymptotic self-similarity $y_d^{dif} \propto t^{1/4}$, which is reached for large times $t \gtrsim 2$ yrs. This is consistent with the estimated gauge time $\tau_b \leq 30$ d fixed by the application (i.e., $t \gg \tau_b$).
- The $\sqrt{2b}$-magnification of the diffusion induced degradation process through the fracture, highlighted by a perfect alignment of the results along a straight-line in the $y_d^{dif}/\sqrt{2b} \times t^{1/4}$-plot, displayed in figure 4. By linear regression, the numerical results for $t \geq 2$ yrs can be expressed in the form of (17):
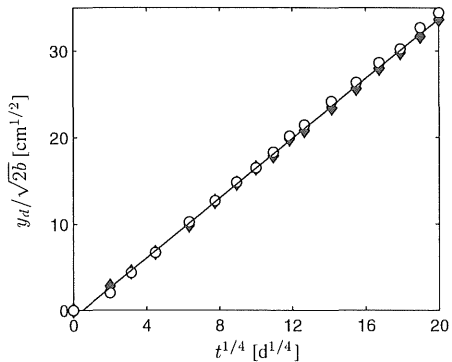
Figure 4: Fracture degradation length $y_d/\sqrt{2b}$ versus $t^{1/4}$ for a pure diffusive mass transport in the fracture, and for different crack openings $2b$: $\bigcirc$ = 0.1 mm and $\blacklozenge$ = 1 mm. The solid line corresponds to the linear regression (30) of data for crack widths 0.1, 0.2, 0.4, 0.6, 0.8, and 1 mm, and times $t > 2$ yrs. [Boundary Condition $\mathcal{B}1$]

$$\frac{y_d^{dif}(t)}{\sqrt{2b}} = 1.73\,t^{1/4} - 0.84 \qquad (21)$$

with y_d^{dif} and $2b$ in cm, and time t in days.

The asymptotic solution (17), therefore, still holds despite the non-linearity of porosity $\phi = \phi(s)$, diffusivity $D_{eff} = D_{eff}(\phi)$, and chemical equilibrium condition $s = g(c)$, that characterize 'real' calcium leaching. It can be employed for assessing the Portlandite dissolution front, when replacing the diffusivity of the solid matrix (D_m) and the porosity (ϕ) in (17) by the values of the same parameters of the undegraded material.

Finally, from a practical point of view, the confirmed asymptotic behavior suggests —for large times— an insignificant acceleration of the bulk material degradation through the diffusion dominated mass transfer in the fracture, in comparison with a 1D-dissolution process that originates from the boundary at $x = 0$. This is illustrated in figure 3, in which the solid line represents the front position of the 1D-dissolution process through the bulk material (similarly to Eq. (14)). As time increases, the 1D-degradation process, which evolves with the square root of time, reaches and overtakes the fracture degradation length $y_d^{dif}(t)$ evolving with the quadratic root of time. This behavior is confirmed through a refined analysis applying boundary conditions $\mathcal{B}2$. The degraded depth $y_d^{dif}(t)/\sqrt{2b}$ versus $t^{1/4}$ is given in figure 5, and need to be compared with figure 4. We note a significant deviation from the asymptotic behavior (21) for times $t \geq 2 - 10$ yrs, depending on the crack opening. This deviation corresponds to the switch from the diffusion-induced degradation through the fracture ($y_d^{dif}(t) \propto t^{1/4}$), to the diffusion-
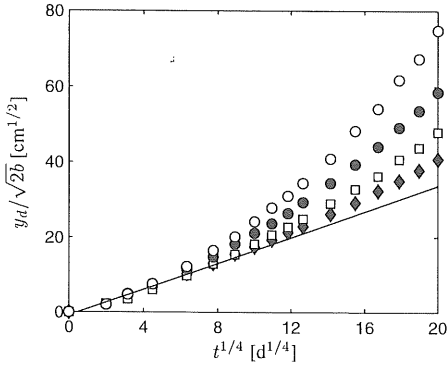
Figure 5: Fracture degradation length $y_d/\sqrt{2b}$ versus $t^{1/4}$ for a pure diffusive mass transport in the fracture, isotropic solid matrix diffusivity, and different crack openings $2b$: ○ = 0.1 mm; ● = 0.2 mm; □ = 0.4 mm; ♦ = 1 mm. The solid line corresponds to the linear regression (30) [Boundary Condition $B2$]

induced degradation through the solid porous material $(y_d(t) \propto t^{1/2})$; and the time for this switch to occur corresponds to the time it takes the 1D-diffusion-dissolution process prevailing in the bulk material to reach the slower $t^{1/4}-$ diffusion in the fracture. This switch can also be depicted from figure 6, which shows the same as figure 5, but now plotted as a function of the square root of time. For large values of time, the degraded depth develops with the same $t^{1/2}$-kinetics (*i.e.* same slopes in figure 6), indicating that the degradation process at the fracture-matrix interface is governed by the one-dimensional diffusive transport prevailing in the bulk material.

From the $\sqrt{2b}-$dependence of the diffusion dominated mass transport in the fracture, it is readily understood that this switch occurs the earlier in time and
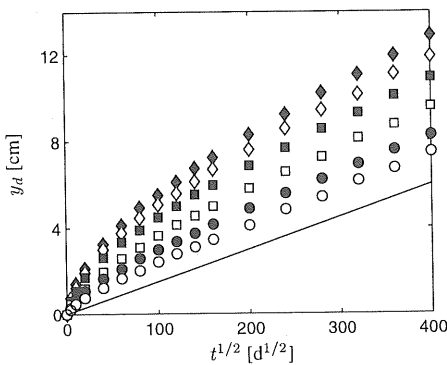

Figure 6: Solid calcium concentrations for a pure diffusive mass transport in the fracture at different times. (Crack width $2b = 0.4$ mm, mesh = 10×12 cm) [Boundary Condition $B2$]

the stronger, the smaller the fracture opening. Therefore, as expected from physical evidence, the smaller

the fracture opening, the less affects a diffusion-dominated mass transport in the fracture the overall degradation process. For large times, the difference between the positions of the degradation fronts along the fracture and in the bulk material becomes constant.

Finally, we should note that there exists another type of $t^{1/2}-$ dependence of the front propagation y_d, which becomes relevant when advective transport in the fracture is taken into account. In this case, for large times, the fracture degradation length evolves according to (Mainguy et al. 2001):

$$t \gg \tau_b: \quad y_d^{adv}(t) = \bar{y}_d^{adv}(\varepsilon) V \frac{2b}{\phi} \left(\frac{t}{D_m} \right)^{1/2} \quad (22)$$

where $\bar{y}_d^{adv}(\varepsilon)$ is the dimensionless front position which depends only on the macroscopic solubility parameter ε; while V is the velocity of the solvent in the crack. However, from model-based simulation we showed that this advective transport in cement-based materials is only relevant for 'high' fluid velocities of $V \geq 8$ cm/d, which corresponds roughly to a Péclet number on the order of $Pe \simeq 80$.

4 CONCLUSIONS

1. Diffusion dominated mass transfer in fractures does not significantly increase the material degradation. The propagation of the fracture degradation length develops with the quadratic root of time, until the faster $t^{1/2}-$front propagation through the bulk material catches up with the $t^{1/4}-$degradation process in the fracture. This shift in self-similarity occurs the earlier the smaller the fracture width, in cracked porous materials with fractures of aspect ratios $L_y/2b > 200$ (estimated from (21) and the solution of the 1D-calcium leaching process). For smaller fracture aspect ratio, a solute congestion will occur in the fracture: the diffusion in the fracture is too slow to evacuate the mineral dissolved in the adjacent porous materials to the outside.

2. While this paper focusses on the effect of cracks and fractures on the demineralization process, it is of interest to evaluate inversely the effect of the leaching process on crack propagation. For instance, for a given structure of size $\mathcal{L}$, Irwin's number $\mathcal{I}$ provides a first estimate of the extent of the fracture process zone ℓ, and therefore of the brittleness or ductility of the fracture:

$$\mathcal{I} = \left(\frac{\mathcal{L}}{\ell} \right)^{1/2} \propto \frac{f_t \mathcal{L}^{1/2}}{(EG_f)^{1/2}} \quad (23)$$

Here, f_t is the tensile strength, E the Young's

modulus, and G_f the fracture energy. Therefore, for the same structure of size $\mathcal{L}$, the ratio of Irwin's number before ($\mathcal{I}_0 \propto \ell_0^{-1/2}$) and after degradation ($\mathcal{I}_\infty \propto \ell_\infty^{-1/2}$) is inversely proportional to the square-root of the fracture-process zone length ratio:

$$\left(\frac{\mathcal{I}_0}{\mathcal{I}_\infty}\right) \sim \left(\frac{f_{t0}}{f_{t\infty}}\right) \times \left(\frac{E_\infty}{E_0}\right)^{1/2} \times \left(\frac{G_{f\infty}}{G_{f0}}\right)^{1/2} \tag{24}$$

The strength decrease ("chemical softening") due to calcium leaching is on the order of 90% (Heukamp et al. 2001), and the loss of elastic stiffness ("chemical damage") on the order of 60% (Bellégo 2001), thus:

$$\frac{\ell_\infty}{\ell_0} \approx 40 \times \left(\frac{G_{f\infty}}{G_{f0}}\right) \tag{25}$$

A pessimistic estimate for G_f is that it evolves proportional to $G_f \propto f_t^2/E$, and an optimistic one is that G_f evolves in the same way as the energy release rate G, which in turn is roughly proportional to the Young's modulus, i.e. $G_f \propto E$. The lower bound leads to $\ell_\infty/\ell_0 \gtrsim 1$, while the second case, which is consistent with Le Bellego's three point bending data on degraded notched beams (Bellégo 2001), leads to $\ell_\infty/\ell_0 \lesssim 16$. Hence, it is expected that the fracture process zone ℓ increases due to chemical degradation, which suggests that the degraded material behaves more ductile than the undegraded one.

ACKNOWLEDGEMENTS

REFERENCES

Adenot, F. and M. Buil (1992). Modelling of the corrosion of the cement by deionized water. *Cement and Concrete Research 22*(4), 451–457.

Adenot, F., B. Gérard, and J. Torrenti (1999). Etat de l'art. In J. Torrenti, O. Didry, J. Olivier, and F. Plas (Eds.), *La dégradation des bétons*, communications en mécanique, pp. 19–46. Hermes, Paris.

Bellégo, C. L. (2001). *Couplages chimie - mécanique dans les structures en béton attaquées par l'eau: étude expérimentale et analyse numérique*. PhD dissertation, ENS Cachan, France. In French.

Berner, U. (1988). Modelling the incongruent dissolution of hydrated cement minerals. *Radiochimica Acta* (44), 387–393.

Heukamp, F., F.-J. Ulm, and J. Germaine (2001). Mechanical properties of calcium leached cement pastes: Triaxial stress states and the influence of the pore pressure. *Cement and Concrete Research*. Accepted for publication.

Hughes, T. (1987). *The Finite Element Method. Linear Static and Dynamic Finite Element Analysis, 2nd edition*. Prentice Hall.

Mainguy, M. and O. Coussy (2000). Propagation fronts during calcium leaching and chloride penetration. *ASCE J.Engrg. Mech. 126*(3), 250–257.

Mainguy, M. and F.-J. Ulm (2001). Coupled diffusion-dissolution around a fracture channel: the solute congestion phenomeno. *Transport in Porous Media*. Accepted for Publication.

Mainguy, M., F.-J. Ulm, and F. Heukamp (2001). Similarity properties of demineralization and degradation of cracked porous materials. *International Journal of Solids and Structures*. Accepted for Publication.

Reardon, E. (1992). Problems and approaches to the prediction of the chemical composition in cement/water system. *Waste Management 12*, 221–239.

Sun, N. (1996). *Mathematical Modeling of Groundwater Pollution*. Springer.

Tognazzi, C. (1998). *Couplage fissuration-dématériaux cimentaires: Caractérisation et modélisation*. PhD dissertation, INSA Toulouse, France. In French.

Walton, J. and R. Seitz (1992). Fluid flow through fractures in below ground concrete vaults. *Waste Management 12*, 179–187.